HHS Public Access

Author manuscript

Cancer Gene Ther. Author manuscript; available in PMC 2015 July 01.

Published in final edited form as:

Cancer Gene Ther. 2015 January ; 22(1): 1–8. doi:10.1038/cgt.2014.58.

Genetic Modification of Neurons to Express Bevacizumab for Local Anti-angiogenesis Treatment of Glioblastoma

Martin J. Hicks, PhD[#1], **Kosuke Funato, PhD**[#2], **Lan Wang, PhD**[1], **Eric Aronowitz, MD**[3], **Jonathan P. Dyke, PhD**[3], **Douglas J. Ballon, PhD**[3], **David F. Havlicek, BS**[1], **Esther Z. Frenk, BS**[1], **Bishnu P. De, PhD**[1], **Maria J. Chiuchiolo, PhD**[1], **Dolan Sondhi, PhD**[1], **Neil R. Hackett, PhD**[1], **Stephen M. Kaminsky, PhD**[1], **Viviane Tabar, MD**[2,†], and **Ronald G. Crystal, MD**[1,†]

[1]Department of Genetic Medicine Weill Cornell Medical College, New York, New York
[2]Department of Neurosurgery Memorial Sloan-Kettering Cancer Center, New York, New York and
[3]Department of Radiology Weill Cornell Medical College, New York, New York

[#] These authors contributed equally to this work.

Abstract

The median survival of glioblastoma multiforme (GBM) approximately 1 yr. Following surgical removal, systemic therapies are limited by the blood-brain barrier. To circumvent this, we developed a method to modify neurons with the genetic sequence for therapeutic monoclonal antibodies using adeno-associated virus (AAV) gene transfer vectors, directing persistent, local expression in the tumor milieu. The human U87MG GBM cell line or patient-derived early passage GBM cells were administered to the striatum of NOD/SCID immunodeficient mice.

AAVrh.10BevMab, an AAVrh.10-based vector coding for bevacizumab (Avastin®), an anti-human vascular endothelial growth factor (VEGF) monoclonal antibody, was delivered to the area of the GBM xenograft. Localized expression of bevacizumab was demonstrated by quantitative PCR, ELISA and Western. Immunohistochemistry showed the bevacizumab was expressed in neurons. Concurrent administration of AAVrh.10BevMab with the U87MG tumor reduced tumor blood vessel density, and tumor volume and increased survival. Administration of AAVrh. 10BevMab 1 wk after U87MG xenograft reduced growth and increased survival. Studies with patient-derived early passage GBM primary cells showed a reduction in primary tumor burden with an increased survival. This data supports the strategy of AAV-mediated CNS gene therapy to treat GBM, overcoming the blood-brain barrier through local, persistent delivery of an anti-angiogenesis monoclonal antibody.

Correspondence: Department of Genetic Medicine Weill Cornell Medical College 1300 York Avenue, Box 164 New York, New York 10065 Phone: (646) 962-4363 Fax: (646) 962-0220 geneticmedicine@med.cornell.edu.
[†]Co-senior authors

Conflict of Interest: None

Keywords

glioblastoma; blood-brain barrier; gene therapy; adeon-associated virus; bevacizumab

Introduction

Glioblastoma multiforme (GBM), the most common central nervous system (CNS) malignancy, is an aggressive human cancer, with a median survival of about 14 months [1-3]. Current therapy includes a combination of surgery, radiation and chemotherapy, but the invasive growth of the tumor prevents complete removal, and GBM is typically radioresistant [4-6]. Although a great deal is known about the aberrant biology exhibited by GBM, applying therapies against these biologic processes is limited by the blood-brain barrier which restricts many systemically administered therapies from reaching the brain parenchyma, including anti-cancer monoclonal antibodies [7-12]. Based on the knowledge that GBM are highly vascular, and express high levels of the angiogenic mediator vascular endothelial growth factor (VEGF) there have been several clinical studies of systemically administered anti-VEGF monoclonal antibodies, but the results have been disappointing, with little effect on the survival from GBM [9,13].

While several hypotheses have been proposed as to the mechanism of bevacizumab resistance in recent clinical trials [14,15], maintenance of therapeutic levels behind the blood-brain barrier is a major concern that has not been fully addressed. This is particularly concerning in areas of that fail to display (MRI) contrast enhancement and therefore the blood-brain barrier is presumed intact. We hypothesize that the impact of anti-VEGF therapy could be best harnessed if persistent local CNS therapeutic levels of anti-VEGF antibody could be readily achieved.

We propose to bypass the blood-brain barrier to anti-VEGF monoclonal antibody therapy by using adeno-associated virus (AAV) gene transfer vectors to deliver the genetic sequences for monoclonal antibodies directly to neurons, thus enlisting normal CNS cells for long term delivery of therapeutic monoclonal antibodies in the local milieu. The clinical strategy would be to surgically remove as much of the tumor as possible, and at the same time, administer to the local area an AAV vector encoding the therapeutic antibody. Because neurons do not turn over, the expression of the monoclonal would be persistent, an important feature for treating GBM, where it is not feasible to surgically remove the entire tumor [4,6]. Based on our experience in delivering genes to the CNS for other applications, we chose the AAVrh.10 vector, as it has the property of mediating excellent CNS expression specifically in neurons, and has been shown to be safe in studies of CNS gene transfer [16-19].

With this background, the present study evaluates the effectiveness of AAVrh.10BevMab, an AAVrh.10 gene transfer vector coding for bevacizumab (Avastin®), to suppress the growth of human GBM in the CNS of immunodeficient mice. The data demonstrates that AAVrh.10BevMab mediates expression of bevacizumab in CNS neurons, and reduces GBM tumor burden as shown by histology, magnetic resonance imaging and increased survival.

Methods

Recombinant AAVrh.10 Vectors

The AAVrh.10BevMab vector is based on the non-human primate-derived rh.10 capsid pseudotyped with AAV2 inverted terminal repeats surrounding the anti-VEGF antibody expression cassette. The expression cassette consists of the cytomegalovirus (CMV) enhancer-chicken– β-actin promoter, the bevacizumab monoclonal heavy chain coding sequence, a 4-amino-acid furin cleavage site and the 24-amino-acid self-cleaving 2A peptide, the bevacizumab light chain coding sequence, and the rabbit β-globin polyadenylation signal [20-22]. The cDNA sequence of the VEGF antibody heavy chain (IgG1) and light chain (κ chain) were as previously described [23]. The negative control vector AAVrh.10anticoc.Mab (referred to as “AAVcontrol”) encodes an irrelevant antibody directed against cocaine [24]. The production and characterization of AAVrh.10BevMab is detailed in Supplementary Materials and Methods.

Murine Experimental Animal Model of GBM Delivery

U87MG (American Type Culture Collection, Manassas, VA) glioblastoma cells were cultured in Eagle's Minimum Essential Medium in fetal bovine serum (10%). Low passage primary human glioblastoma cells (0709) were cultured in DMEM/F12 with epidermal growth factor and basic fibroblast growth factor each at 20 ng/ml on 10 cm plates (BD Biosciences, San Jose, CA) that have been coated with poly-L-ornithine (1:1000 of 15 mg/ml), laminin (1:250 of 1 mg/ml, R&D Systems, Minneapolis, MN) and fibronectin (1:500 of 1 mg/ml, BD Biosciences).

The most likely clinical use of AAVrh.10BevMab for treatment of glioblastoma would be to remove as much tumor as possible, and after tumor removal at the time of surgery, to administer the AAVrh.10BevMab vector in the local CNS region. Based on the knowledge that AAVrh.10BevMab express bevacizumab within 1 wk, and the local expression of bevacizumab would contribute to suppression of growth of residual tumor cells left post-surgery, AAVrh.10BevMab therapy or controls (PBS or an AAVrh.10 vector coding for an irrelevant antibody) were administered to the CNS simultaneously with the tumor cells or 6 days after implantation of the tumor cells.

Female NOD/SCID immunodeficient mice, 6 to 8 wk old (Jackson, Bar Harbor, ME) were housed under pathogen-free conditions. At 7 to 10 wk of age the mice were treated with PBS, AAVrh.10BevMab or AAVcontrol at 10^{11} genome copies (gc) by direct CNS administration in 2 to 5 μl. CNS administration to the right hemisphere of the tumor cells and the vector were administered stereotaxically in the lower striatum (A/P +1.0 mm, M/L ±1.0 mm, D/V - 3.0 mm), at a rate of 0.5 μl/min using a 10 μl syringe (Hamilton, Reno, NV) with a 26 g needle. The needle was left in position for 2 min before and 2 min following administration, at which point it was withdrawn slightly (1 mm) and left for 1 min, and then fully withdrawn over the course of an additional minute. For the concurrent administration of U87MG tumor cells and therapy, 10^5 cells were administered in a total volume of 2 μl together with 10^{11} gc AAVrh.10BevMab or control (AAVrh.10 vector coding for an irrelevant antibody or PBS) in a volume of 3 μl (total volume 5 μl). For the U87MG cells

treated 6 days after tumor administration, 10^5 U87MG cells were administered in a volume of 2 μl, followed 6 days later by 10^{11} gc AAVrh.10BevMab in a volume of 2 μl. For the 0709 low passage primary cells, 10^5 cells were administered in a total volume of 3 μl together with 10^{11} gc AAVrh.10BevMab or control (AAVrh.10 vector coding for an irrelevant antibody or PBS) in a volume of 3 μl (total volume 6 μl). Mice were sacrificed at time point indicated or upon signs of neurological impairment, cachexia, or significant loss of weight (decrease in 1/3 adult body weight). All animal studies were conducted under protocols reviewed and approved by the Weill Cornell Institutional Animal Care and Use Committee.

Quantification of Bevacizumab

Samples of brain and organ tissue were collected after perfusion with cold phosphate buffered saline (PBS, pH 7.4). Coronal sections of mouse brain divided the 2 hemispheres into 4 segments (equidistance anterior to posterior). The levels of bevacizumab mRNA were assessed by RNA reverse transcription and TaqMan quantitative PCR (Applied Biosystems). Levels of bevacizumab antibody were determined by ELISA and Western, and cell localization of bevacizumab expression assessed by immunohistochemistry (see Supplementary Materials and Methods for details).

Magnetic Resonance Imaging Quantification

Magnetic Resonance Imaging was performed on a 7.0 Tesla 70/30 Bruker Small Animal MRI scanner (Bruker Biospin, Bilerica, MA) equipped with an additional small animal imaging gradient set (45 G/cm). Animals were imaged under isoflurane anesthesia (2% to initiate anesthesia, 1% for maintenance). A warming bed was used to maintain a constant body temperature and respiration was also monitored throughout the imaging procedure.

High-resolution imaging sequences were acquired prior to and following tail vein administration of the MRI contrast agent, gadopentetate dimeglumine (Gd-DTPA; Berlex Laboratories; Wayne, NJ; 8 nmol/mouse in 40 μl volume). A T1-Weighted 2D FLASH sequence was used to visualize contrast enhancement with a repetition time of 357 ms and an echo time of 3.8 ms. T2-Weighted Turbo RARE sequences were also acquired with repetition and echo times of 2300 ms/48 ms, respectively, to detect edema. A 20 mm field of view and 256 x 256 matrix produced an image resolution of 78 μm x 78 μm x 500 μm with 20 matching axial slices.

Tumor burden was assessed for the U87GM line T1(Gd-DTPA enhanced) and T2 weighted sequences using IDL 8.1 custom coded algorithms (Exelis Visual; Boulder, CO). For the U87MG tumor burden, tumor volume (ml) was assessed using T1 Gd-DTPA enhanced) sequences of the demarcated tumor. For the 0709 primary tumor, tumor burden was assessed using T2 weighted sequences. Given the diffuse nature of the 0709 tumor, tumor burden was calculated on the whole brain volume (ml), by outlining the perimeter of mouse brain.

Statistics

Data are expressed as means ± standard error, and comparisons between groups were conducted by a two-tailed unpaired t-test, comparisons between treatment groups at multiple

time points were conducted by two-way analysis of variance (MedCalc Software,Ostend, Belgium) The survival data was generated using Kaplan-Meier survival plot and groups were compared using the Mantel-Cox test (GraphPad Software, Inc., La Jolla, CA).

Results

The area of AAVrh.10BevMab CNS administration was compared to other regions of the CNS to assess bevacizumab mRNA and protein levels in and around the targeted region and absence in the non-targeted left hemisphere and posterior regions of the CNS (Figure 1A). Regional sections of the mouse brain and peripheral organs assayed by reverse transcription quantitative PCR showed AAVrh.10BevMab-directed expression of bevacizumab mRNA in the targeted region of the right hemisphere to be significantly greater (more than 8-fold) than the highest level observed in the left hemisphere (L2) and significantly greater (more than 10-fold) than the highest levels of a peripheral organ, the liver, with much lower levels in other organs ($n=3$; $p<0.01$; Figure 1B). Detection of expressed bevacizumab protein levels by ELISA and analysis of total protein showed localized expression of the bevacizumab monoclonal antibody in the area of the administration ($n=4$; Figure 1C). The targeted area of the right striatum showed the highest expression among the sections at 2 wk, with increased levels at 6 wk, the last time point measured. There was minimal expression in posterior regions and opposite (left) hemisphere of the mouse brain. Importantly, significantly lower or below limit of detection levels of bevacizumab mRNA were measured in non-targeted peripheral organs (liver, lung, heart and kidney) and blood ($p<0.01$; Figure 1B). Likewise, only minimal bevacizumab protein was found in the blood (50-fold less than the injected region of the brain; $p<0.02$; Figure 1C).

Immunohistochemical assessment of the CNS showed AAVrh.10BevMab-directed expression of bevacizumab in the area of administration. Coronal sections taken at 1 mm anterior of the bregma near the approximate site of AAVrh.10BevMab administration were examined for expression of bevacizumab and its association with either astrocytes (glial cells) or neurons (Figure 1D) [16]. Counter-staining of glial cells showed that glial cells were not associated with bevacizumab expression, while counter-staining of neurons showed colocalization and adjacent staining of neurons with bevacizumab (Figure 1D), demonstrating an association between neurons and AAVrh.10BevMab expression of the therapeutic antibody. The merged image of glial and neuronal staining demonstrates AAVrh. 10 specificity for neurons, but not glial cells (Figure 1D).

In a first set of experiments, NOD/SCID mice received U87MG cells and the AAVrh. 10BevMab vector concurrently. The control groups received tumor cells and PBS instead of the viral vector. Animals underwent serial MRI imaging and were assessed for tumor volume and sacrificed upon evidence of significant cachexia or neurological impairment. Upon sacrifice, the brain tissue was assessed for vascular density as evidence for neo-angiogenesis, as well as tumor histology. All animals had evidence of surviving tumor cells with distinct borders (Figure 2A). Immunohistochemistry (IHC) for the endothelial marker CD31 demonstrated a substantial decrease in blood vessel density in the tumor area of AAVrh.10BevMab-treated mice, compared to PBS controls ($n=3$, $p<0.05$, Figure 2B,C).

The vessels seen in the AAVrh.10BevMab treated animals display a more normal morphology as compared to the large sinusoidal vessels seen in the untreated tumors.

Serial MRI imaging using Gd-DTPA enhancement demonstrated a progressive increase in tumor volume in the untreated mice while the treated group exhibited reduced tumor growth by greater than 5-fold at 18 days post injection (Figure 3a-b). To more closely approximate the clinical setting, a second group of mice received tumor cell implants followed 6 days later by administration of the AAVrh.10BevMab vector. The animals were monitored and assessed by MRI as with the previous group. The results were similar to the group with concurrent administration. MRI showed a statistically significant 2.4-fold decrease in tumor volume at 20 days (n=4, AAVrh.10BevMab post-xenograft treated *vs* AAVcontrol, $p<0.04$; Figure 3C,D).

Survival data demonstrated a statistically significant increase in survival time in mice that received the AAVrh.10BevMab vector in both experimental strategies (concurrent and post-xenograft). Concurrent treatment with AAVrh.10BevMab increased the median survival time of mice with GBM xenografts by 42% (n=9, AAVrh.10BevMab treated *vs* AAVcontrol, $p<0.003$; Figure 4A), while treatment post tumor establishment led to a larger 64% increase in survival (n=6, AAVrh.10BevMab post-xenograft treated *vs* AAVcontrol, $p<0.004$; Figure 4B).

A similar experimental paradigm was repeated in NOD/SCID mice implanted with GBM cells obtained from a freshly dissociated patient tumor and passaged briefly in serum-free media. MRI analysis over time showed a reduced tumor burden in the treatment group (Figure 5A). MRI volumetric assessment showed a reduction in primary tumor burden by 3.3-fold at 12 wk in the treated group (n=3, treated *vs* control-treated, $p<0.002$ Figure5A). Survival was also extended in the AAVrh.10BevMab group through wk 15 (n=21, treated *vs* control-treated, $p<0.006$; Figure 5B).

Tissue analysis demonstrated large infiltrating tumors in the control group while the AAVrh.10BevMab treated mice showed clusters of tumor growing in areas well beyond the site of AAV administration. Immunohistochemistry demonstrated the absence of bevacizumab antibody secretion in areas of tumor growth, with few single cells infiltrating around the area of vector administration (n=3; Figure 5C). Interestingly, tumor cells growing in the AAVrh.10BevMab treated animals demonstrated an increase in the expression of phosphorylated c-Met, which has been proposed recently to represent an evasive mechanism in response to anti-angiogenic inhibition (n=3; Figure 5D) [25].

Discussion

The blood brain barrier represents a major challenge in the development of an effective therapy directed toward glioblastoma, as it restricts systemically administered large molecules from reaching the targeted area in the brain. While the blood-brain barrier can be permeable in areas of high neo-angiogenesis and leaky vasculature, these “contrast-enhancing” regions are frequently the target of debulking surgery [26,27]. However, tumor cells are known to persist in an infiltrative fashion in the surrounding regions, usually in

areas where the blood-brain barrier is intact (non-contrast enhancing regions). These cells are frequently responsible for tumor recurrence and are more difficult to target with conventional therapies.

By direct administration of the AAVrh.10BevMab vector to the CNS of immunodeficient mice with human GBM, we have bypassed the blood-brain barrier to deliver to neurons the genetic code for the monoclonal antibody bevacizumab. The data demonstrates persistent expression of bevacizumab resulting in reduced tumor blood vessel density in the area of tumor, a significant reduction in tumor growth and a significant increase in survival in both concurrent and post-xenograft models. AAV-mediated gene transfer of therapeutic monoclonal antibodies directly to the CNS overcomes a common hurdle to anti-tumor therapy, the blood-brain barrier, and through local and persistent expression, provides an effective barrier to neo-angiogenesis.

Glioblastoma Multiforme

GBM accounts for the majority of all primary brain tumors [1-3]. Despite advances in the molecular and physiological characterization of GBM, the median overall survival of GBM patients remains little more than one year. The standard therapy to increase survival in GBM patients consists of maximal surgery followed by radiation and various chemotherapy agents. Nonetheless these tumors are remarkably resistant to both radiation [4-6] and chemotherapy and typically recur within months of treatment [28,29].

GBM is distinguished by prominent vascular proliferation, and rapid and invasive growth, and was thus thought to be a prime target for anti-angiogenesis inhibitors. The introduction of bevacizumab to the clinic was met with initial excitement, as normalization of the vessels by this agent leads to significant palliation of symptoms related to leaky vessels and cerebral edema. However, recent data indicate that the response of GBM to bevacizumab in humans is relatively short-lived, with emerging evidence of tumor refractoriness and no significant impact on overall survival [30].

The mechanisms of this failure remain unclear, but several possibilities have been proposed [31]. Those include the amplification of pro-angiogenic genes in resistant tumors, thus requiring higher doses of anti-angiogenic treatment, or an escape to a different mode of angiogenesis such as vasculogenesis [32]. Alternative mechanisms of angiogenesis, including the Notch pathway, or a transition to a more invasive phenotype have also been suggested [25,33]. However, studies show that disruption of the blood brain barrier can enhance permeability to drugs like bevacizumab therefore a key element pertaining to the failure of bevacizumab in the clinic could be the degree of penetration across the blood brain barrier, especially in areas of relatively normal vasculature [10]. Although studies of angiogenic growth and proliferation pathways of primary tumors has uncovered GBM sensitive targets, the systemic delivery of immunotherapies to block these targets in GBM clinical trials has not increased survival [7,8,11,12,34,35]. The disadvantage of current GBM therapy with monoclonal antibodies is the necessity for repeat administration delivered by the intravascular route and at high dose, resulting in systemic distribution of the therapeutic monoclonal antibody [35,36]. Although the targeted area is within the CNS, systemic delivery results in drug distribution to healthy non-targeted organs and there is limited

diffusion of the monoclonal into the tumor [37-39]. AAV-directed gene therapy to the CNS overcomes these challenges, potentially eliminating side-effects while maintaining a long term and effective dose directed at the site of the tumor [17].

Anti-VEGF Therapy for Glioblastoma

GBM is characterized by extensive vasculature and thus is susceptible to angiogenesis inhibitors. Like many other tumors, most GBM produce VEGF, a major inducer of angiogenesis. [8] The classical form of VEGF (VEGF-A), functions through 3 receptors (VEGFR-1, VEGFR-2 and NRP-1) to induce cell growth [40]. Bevacizumab (Avastin®) is an FDA approved humanized monoclonal that blocks VEGF-A [41]. It is an IgG antibody that consists of two identical light chains and two heavy chains with a molecular weight of 150 KD and a diameter of 15 nm (Roche, Data Sheet). In general, IgG molecules have been shown experimentally to be excluded from the brain via the blood-brain barrier, although they can be transported from brain to blood via the FcRn transporter [42,43]. Our strategy thus bypasses the blood-brain barrier, achieves sustained intratumoral therapeutic levels and leads to an augmentation of available drug levels over time. Concomitantly, plasma levels are significantly lower than those achieved in the brain, reducing the potential for systemic side effects.

Bevacizumab is widely used to treat metastatic colon and non-small cell lung cancer, and ocular vascular proliferative disorders [44-47]. Systemic administration of bevacizumab has been tried as a therapeutic for GBM with limited success [9,34,48]. Unlike the application of bevacizumab for the treatment of macular degeneration where bevacizumab is injected directly into the eye [44], the trials for GBM with bevacizumab to date use systemic delivery and thus are limited by the blood-brain barrier in achieving therapeutic levels in the CNS [10,49]. The data in the present study demonstrates a novel mode of delivery showing efficacy with CNS direct delivery of the AAVrh.10BevMab vector to the local area surrounding the tumor xenograft. In the human GBM tumors tested, AAVrh.10BevMab inhibited angiogenesis, reduced tumor growth and increased survival in mice.

In the clinical scenario, AAVrh.10-mediated therapy would be applied at the time of GBM surgical removal. As complete removal is not always feasible, the therapy vector would be administered in the milieu of the excised tumor, and within 1 wk, local neurons would begin expression of a therapeutic dosage of the monoclonal antibody inhibiting GBM recurrence. The stability of neurons would ensure persistent expression of the monoclonal antibody, thereby preventing angiogenesis and proliferation of the remaining tumor cells. In the current study, primary tumor cells survived and proliferated in regions beyond the area of bevacizumab expression, suggesting that the escape mechanism may be related to region of AAVrh.10BevMab administration or dosage rather than resistance. These data suggest that the high persistent levels of AAVrh.10-mediated bevacizumab expressed within tumors are effective to inhibit tumor growth. Furthermore, tumor growth in the treated animals initiated in regions of the brain relatively removed from the area of AAVrh.10BevMab administration. In human translation, AAV vector dose and antibody expression could be modulated to deliver optimal levels of the anti-VEGF monoclonal antibody in critical regions to sufficiently block VEGF sensitive GBM.

Interestingly, the up-regulation of phosphorylated c-Met in AAVrh.10BevMab-treated tumors observed in this study indicates a tumor refractory response due to either low dose bevacizumab within regions of the parenchyma, or alternatively, the selection of subclones of tumor cells with elevated c-Met. Because activation of the c-Met pathway is associated with an increased capacity for invasion and migration, these results suggest the selection of the c-Met subclones in treated tumors. This study illustrates a proof of principle for the strategy of AAV delivery of a monoclonal antibody beyond the blood brain barrier. Future studies that make use of combination treatments, targeting additional tyrosine kinases, such as c-Met, may be necessary for a more effective and significant tumor control. In effect, AAV vectors could be readily modified to encode for distinct monoclonals blocking these and other oncogenic signaling pathways, such as the SDF1/CXCR4 and Notch pathways [32,50]. A combinatorial approach using AAV-monoclonal delivery would favorably alter (and bolster) the therapeutic tumor microenvironment. Our experience with AAV-directed delivery of genes to the CNS has demonstrated that the AAVrh.10 vector mediates an excellent CNS expression profile with specificity for neurons, and has been shown to be safe in studies of CNS gene transfer [16,19]. Efficacy in this study opens the door to future research with adeno-associated virus-mediated delivery of other anti- tumor antibodies in the treatment of glioblastoma and other malignancies within the central nervous system.

Supplementary Material

Refer to Web version on PubMed Central for supplementary material.

Acknowledgments

We thank Stephanie Phillips for help with these studies; N. Mohamed and D.N. McCarthy for help with the manuscript; and Carolyn Wiener for her continued support. These studies were supported, in part, by the Starr Cancer Consortium and the National Foundation for Cancer Research. MJH was supported, in part, by NIH T32HL094284.

References

1. Louis DN, Ohgaki H, Wiestler OD, Cavenee WK, Burger PC, Jouvet A, et al. The 2007 WHO classification of tumours of the central nervous system. Acta Neuropathol. 2007; 114:97–109. [PubMed: 17618441]
2. Van Meir EG, Hadjipanayis CG, Norden AD, Shu HK, Wen PY, Olson JJ. Exciting new advances in neuro-oncology: the avenue to a cure for malignant glioma. CA Cancer J Clin. 2010; 60:166–193. [PubMed: 20445000]
3. Dolecek TA, Propp JM, Stroup NE, Kruchko C. CBTRUS statistical report: primary brain and central nervous system tumors diagnosed in the United States in 2005-2009. Neuro Oncol. 2012; 14(Suppl 5):v1–49. [PubMed: 23095881]
4. Barker FG, Chang SM, Gutin PH, Malec MK, McDermott MW, Prados MD, et al. Survival and functional status after resection of recurrent glioblastoma multiforme. Neurosurgery. 1998; 42:709–720. [PubMed: 9574634]
5. Allahdini F, Amirjamshidi A, Reza-Zarei M, Abdollahi M. Evaluating the prognostic fac tors effective on the outcome of patients with glioblastoma multiformis: does maximal re-section of the tumor lengthen the median survival? World Neurosurg. 2010; 73:128–134. [PubMed: 20860940]
6. Park JK, Hodges T, Arko L, Shen M, Dello ID, McNabb A, et al. Scale to predict survival after surgery for recurrent glioblastoma multiforme. J Clin Oncol. 2010; 28:3838–3843. [PubMed: 20644085]

7. Wang R, Chadalavada K, Wilshire J, Kowalik U, Hovinga KE, Geber A, et al. Glioblastoma stem-like cells give rise to tumour endothelium. Nature. 2010; 468:829–833. [PubMed: 21102433]
8. Knizetova P, Ehrmann J, Hlobilkova A, Vancova I, Kalita O, Kolar Z, et al. Autocrine reg ulation of glioblastoma cell cycle progression, viability and radioresistance through the VEGF-VEGFR2 (KDR) interplay. Cell Cycle. 2008; 7:2553–2561. [PubMed: 18719373]
9. Thompson EM, Frenkel EP, Neuwelt EA. The paradoxical effect of bevacizumab in the therapy of malignant gliomas. Neurology. 2011; 76:87–93. [PubMed: 21205697]
10. Boockvar JA, Tsiouris AJ, Hofstetter CP, Kovanlikaya I, Fralin S, Kesavabhotla K, et al. Safety and maximum tolerated dose of superselective intraarterial cerebral infusion of bevacizumab after osmotic blood-brain barrier disruption for recurrent malignant glioma. Clinical article. J Neurosurg. 2011; 114:624–632. [PubMed: 20964595]
11. Adamson C, Kanu OO, Mehta AI, Di C, Lin N, Mattox AK, et al. Glioblastoma multiforme: a review of where we have been and where we are going. Expert Opin Investig Drugs. 2009; 18:1061–1083.
12. Jain RK, di TE, Duda DG, Loeffler JS, Sorensen AG, Batchelor TT. Angiogenesis in brain tumours. Nat Rev Neurosci. 2007; 8:610–622. [PubMed: 17643088]
13. Sweet JA, Feinberg ML, Sherman JH. The role of avastin in the management of recurrent glioblastoma. Neurosurg Clin N Am. 2012; 23:331–41. x. [PubMed: 22440876]
14. Lai A, Tran A, Nghiemphu PL, Pope WB, Solis OE, Selch M, et al. Phase II study of bevacizumab plus temozolomide during and after radiation therapy for patients with newly diagnosed glioblastoma multiforme. J Clin Oncol. 2011; 29:142–148. [PubMed: 21135282]
15. Zhang G, Huang S, Wang Z. A meta-analysis of bevacizumab alone and in combination with irinotecan in the treatment of patients with recurrent glioblastoma multiforme. J Clin Neurosci. 2012; 19:1636–1640. [PubMed: 23047061]
16. Sondhi D, Hackett NR, Peterson DA, Stratton J, Baad M, Travis KM, et al. Enhanced sur vival of the LINCL mouse following CLN2 gene transfer using the rh.10 rhesus macaque-derived adeno-associated virus vector. Mol Ther. 2007; 15:481–491. [PubMed: 17180118]
17. Sondhi D, Johnson L, Purpura K, Monette S, Souweidane MM, Kaplitt MG, et al. Long-term expression and safety of administration of AAVrh.10hCLN2 to the brain of rats and nonhuman primates for the treatment of late infantile neuronal ceroid lipofuscinosis. Hum Gene Ther Methods. 2012; 23:324–335. [PubMed: 23131032]
18. Worgall S, Sondhi D, Hackett NR, Kosofsky B, Kekatpure MV, Neyzi N, et al. Treatment of late infantile neuronal ceroid lipofuscinosis by CNS administration of a serotype 2 adeno-associated virus expressing CLN2 cDNA. Hum Gene Ther. 2008; 19:463–474. [PubMed: 18473686]
19. Souweidane MM, Fraser JF, Arkin LM, Sondhi D, Hackett NR, Kaminsky SM, et al. Gene therapy for late infantile neuronal ceroid lipofuscinosis: neurosurgical considerations. J Neurosurg Pediatr. 2010; 6:115–122. [PubMed: 20672930]
20. Fang J, Qian JJ, Yi S, Harding TC, Tu GH, VanRoey M, et al. Stable antibody expression at therapeutic levels using the 2A peptide. Nat Biotechnol. 2005; 23:584–590. [PubMed: 15834403]
21. Watanabe M, Boyer JL, Crystal RG. AAVrh.10-mediated genetic delivery of bevacizumab to the pleura to provide local anti-VEGF to suppress growth of metastatic lung tumors. Gene Ther. 2010; 17:1042–1051. [PubMed: 20596059]
22. Mao Y, Kiss S, Boyer JL, Hackett NR, Qiu J, Carbone A, et al. Persistent suppression of ocular neovascularization with intravitreal administration of AAVrh.10 coding for bevacizumab. Hum Gene Ther. 2011; 22:1525–1535. [PubMed: 21801028]
23. Watanabe M, Boyer JL, Hackett NR, Qiu J, Crystal RG. Genetic delivery of the murine equivalent of bevacizumab (avastin), an anti-vascular endothelial growth factor monoclonal antibody, to suppress growth of human tumors in immunodeficient mice. Hum Gene Ther. 2008; 19:300–310. [PubMed: 18324912]
24. Rosenberg JB, Hicks MJ, De BP, Pagovich O, Frenk E, Janda KD, et al. AAVrh.10-mediated expression of an anti-cocaine antibody mediates persistent passive immunization that suppresses cocaine-induced behavior. Hum Gene Ther. 2012; 23:451–459. [PubMed: 22486244]

25. Lu KV, Chang JP, Parachoniak CA, Pandika MM, Aghi MK, Meyronet D, et al. VEGF inhibits tumor cell invasion and mesenchymal transition through a MET/VEGFR2 com plex. Cancer Cell. 2012; 22:21–35. [PubMed: 22789536]
26. Hasselbalch, B.; Lassen, U.; Poulsen, HS. Patients with Recurrent High-Grade Glioma: Thera py with Combination of Bevacizumab and Irinotecan.. In: Hayat, MA., editor. Tumors of the Central Nervous System. Springer Science+Business Media; New York: 2011. p. 289-99.
27. Hawkins-Daarud A, Rockne RC, Anderson AR, Swanson KR. Modeling Tumor-Associated Edema in Gliomas during Anti-Angiogenic Therapy and Its Impact on Imageable Tumor. Front Oncol. 2013; 3:66. [PubMed: 23577324]
28. Nagasawa DT, Chow F, Yew A, Kim W, Cremer N, Yang I. Temozolomide and other potential agents for the treatment of glioblastoma multiforme. Neurosurg Clin N Am. 2012; 23:307–22. ix. [PubMed: 22440874]
29. Chaudhry NS, Shah AH, Ferraro N, Snelling BM, Bregy A, Madhavan K, et al. Predictors of long-term survival in patients with glioblastoma multiforme: advancements from the last quarter century. Cancer Invest. 2013; 31:287–308. [PubMed: 23614654]
30. Arrillaga-Romany I, Reardon DA, Wen PY. Current status of antiangiogenic therapies for glioblastomas. Expert Opin Investig Drugs. 2014; 23:199–210.
31. Norden AD, Drappatz J, Wen PY. Antiangiogenic therapies for high-grade glioma. Nat Rev Neurol. 2009; 5:610–620. [PubMed: 19826401]
32. Kioi M, Vogel H, Schultz G, Hoffman RM, Harsh GR, Brown JM. Inhibition of vasculogenesis, but not angiogenesis, prevents the recurrence of glioblastoma after irradia tion in mice. J Clin Invest. 2010; 120:694–705. [PubMed: 20179352]
33. Li JL, Sainson RC, Oon CE, Turley H, Leek R, Sheldon H, et al. DLL4-Notch signaling mediates tumor resistance to anti-VEGF therapy in vivo. Cancer Res. 2011; 71:6073–6083. [PubMed: 21803743]
34. Pope WB, Xia Q, Paton VE, Das A, Hambleton J, Kim HJ, et al. Patterns of progression in patients with recurrent glioblastoma treated with bevacizumab. Neurology. 2011; 76:432–437. [PubMed: 21282590]
35. von BL, Brucker D, Tirniceru A, Kienast Y, Grau S, Burgold S, et al. Bevacizumab has differential and dose-dependent effects on glioma blood vessels and tumor cells. Clin Can cer Res. 2011; 17:6192–6205.
36. Ebos JM, Pili R. Mind the gap: potential for rebounds during antiangiogenic treatment breaks. Clin Cancer Res. 2012; 18:3719–3721. [PubMed: 22679177]
37. Mancuso MR, Davis R, Norberg SM, O'Brien S, Sennino B, Nakahara T, et al. Rapid vas cular regrowth in tumors after reversal of VEGF inhibition. J Clin Invest. 2006; 116:2610–2621. [PubMed: 17016557]
38. Pitz MW, Desai A, Grossman SA, Blakeley JO. Tissue concentration of systemically ad ministered antineoplastic agents in human brain tumors. J Neurooncol. 2011; 104:629–638. [PubMed: 21400119]
39. Agarwal S, Manchanda P, Vogelbaum MA, Ohlfest JR, Elmquist WF. Function of the blood-brain barrier and restriction of drug delivery to invasive glioma cells: findings in an orthotopic rat xenograft model of glioma. Drug Metab Dispos. 2013; 41:33–39. [PubMed: 23014761]
40. Ferrara N, Hillan KJ, Gerber HP, Novotny W. Discovery and development of bevacizumab, an anti-VEGF antibody for treating cancer. Nat Rev Drug Discov. 2004; 3:391–400. [PubMed: 15136787]
41. Homsi J, Daud AI. Spectrum of activity and mechanism of action of VEGF/PDGF inhibitors. Cancer Control. 2007; 14:285–294. [PubMed: 17615535]
42. Leveque D, Wisniewski S, Jehl F. Pharmacokinetics of therapeutic monoclonal antibodies used in oncology. Anticancer Res. 2005; 25:2327–2343. [PubMed: 16080460]
43. Schlachetzki F, Zhu C, Pardridge WM. Expression of the neonatal Fc receptor (FcRn) at the blood-brain barrier. J Neurochem. 2002; 81:203–206. [PubMed: 12067234]
44. Kourlas H, Abrams P. Ranibizumab for the treatment of neovascular age-related macular degeneration: a review. Clin Ther. 2007; 29:1850–1861. [PubMed: 18035187]

45. Jenab-Wolcott J, Giantonio BJ. Bevacizumab: current indications and future development for management of solid tumors. Expert Opin Biol Ther. 2009; 9:507–517. [PubMed: 19344286]

46. Langer C, Soria JC. The role of anti-epidermal growth factor receptor and anti-vascular en dothelial growth factor therapies in the treatment of non-small-cell lung cancer. Clin Lung Cancer. 2010; 11:82–90. [PubMed: 20199973]

47. Galfrascoli E, Piva S, Cinquini M, Rossi A, La VN, Bramati A, et al. Risk/benefit profile of bevacizumab in metastatic colon cancer: a systematic review and meta-analysis. Dig Liver Dis. 2011; 43:286–294. [PubMed: 21146479]

48. Peak SJ, Levin VA. Role of bevacizumab therapy in the management of glioblastoma. Cancer Manag Res. 2010; 2:97–104. [PubMed: 21188100]

49. Lu JF, Bruno R, Eppler S, Novotny W, Lum B, Gaudreault J. Clinical pharmacokinetics of bevacizumab in patients with solid tumors. Cancer Chemother Pharmacol. 2008; 62:779–786. [PubMed: 18205003]

50. Hovinga KE, Shimizu F, Wang R, Panagiotakos G, Van Der HM, Moayedpardazi H, et al. Inhibition of notch signaling in glioblastoma targets cancer stem cells via an endothelial cell intermediate. Stem Cells. 2010; 28:1019–1029. [PubMed: 20506127]

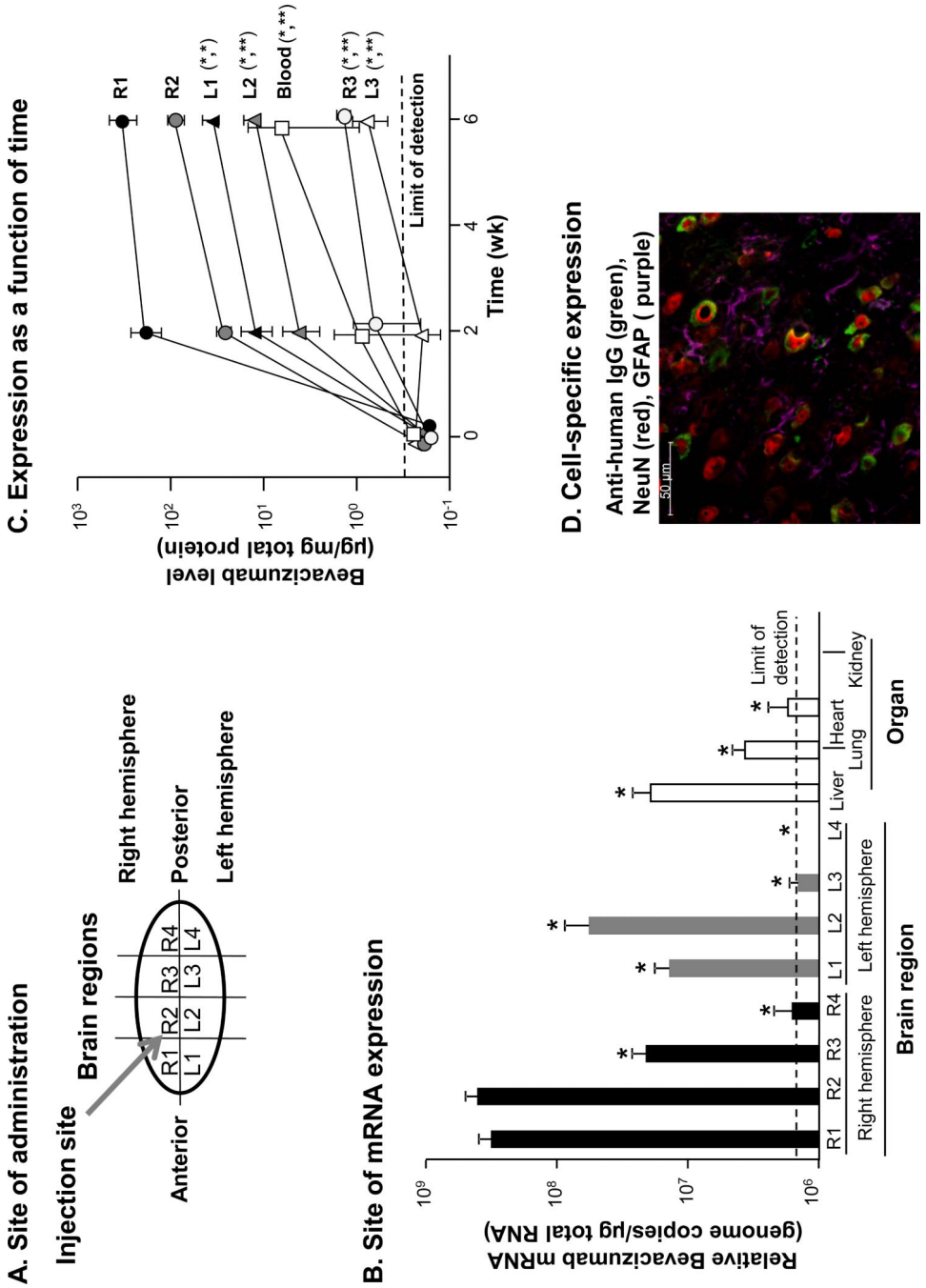

Figure 1.

AAVrh.10BevMab directed expression of bevacizumab in the mouse CNS. **A.** Diagram of the mouse brain illustrates regions for expression analysis and site of vector administration. R = right; L = left**. B.** Relative quantification of AAVrh.10-directed bevacizumab mRNA expression per µg of total RNA in each brain region and in peripheral organs (n=3). The limit of detection denoted by the dashed line. Statistical difference by two tailed t-test to R1 and R2 $p<0.01$ marked with asterisk (*). There was no significant difference between R1 and R2 ($p>0.4$) . **C.** Time-dependent quantification of AAVrh.10-directed bevacizumab

protein expression in each brain region compared to blood (n=4). The limit of detection denoted by the dashed line. R = right; L = left. Statistical difference by two tailed t-test to (R1,R2) $p<0.05$ marked with asterisk (*) and $p<0.01$ (**). **D**.AAVrh.10BevMab-mediated expression of bevacizumab in neurons of the mouse striatum. Shown is immunofluorescent assessment of coronal section of the CNS 4 wk after administration of AAVrh.10BevMab. Detection of AAVrh.10BevMab-directed expression of bevacizumab was assessed with anti-human IgG antibody (anti-IgG, green), glia cells were assessed with anti-glial fibrillary acidic protein (anti-GFAP, purple) and neurons were assessed with neuronal nuclear antigen (NeuN, red). bar = 50 μm.

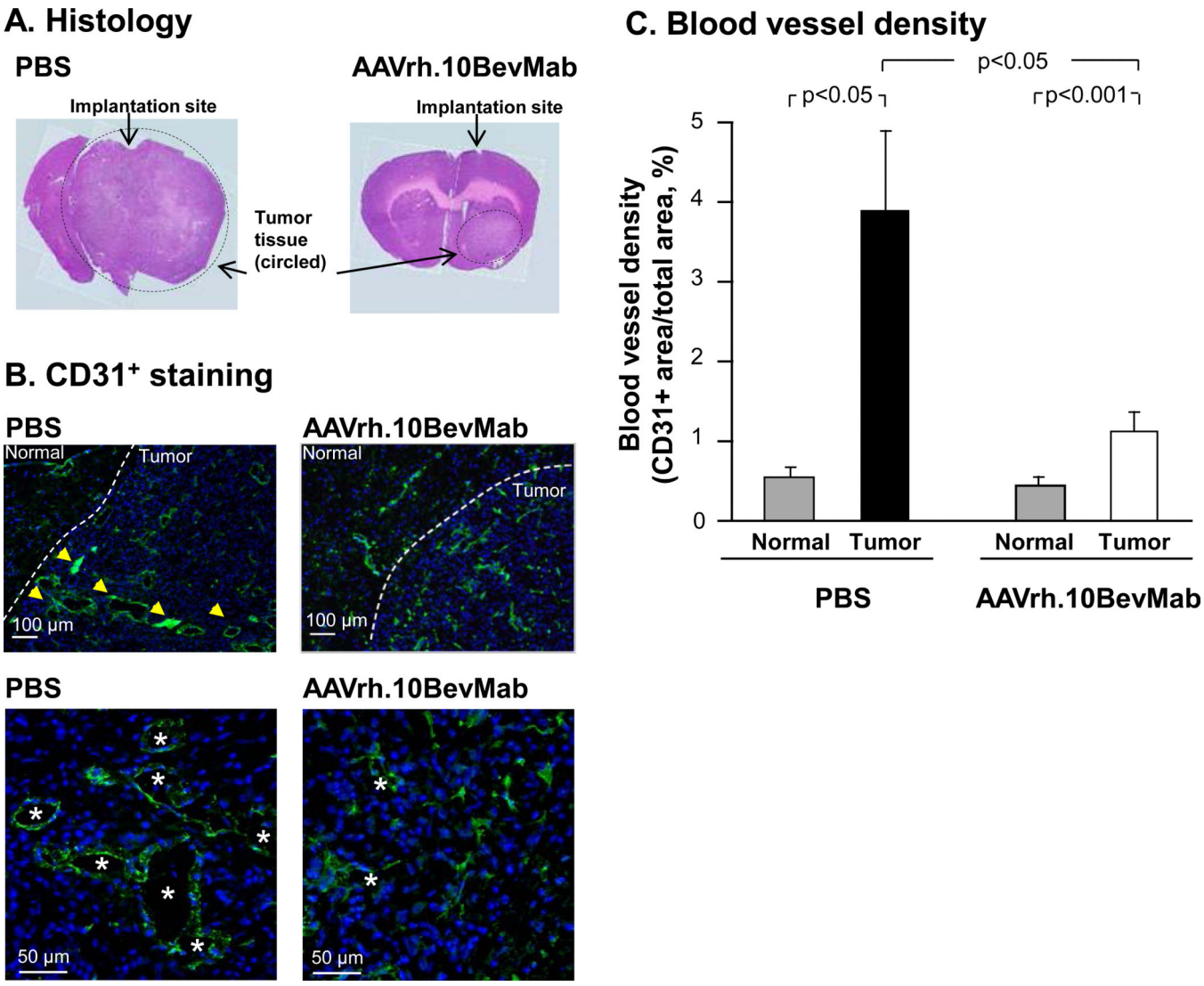

Figure 2.

Histological and immunohistochemical staining of PBS (n=3) *vs* AAVrh.10BevMab-treated (n=3) mouse brains implanted with U87MG tumor. U87MG (10^5 cells) was administered to the right striatum of NOD/SCID immunodeficient mice at the same time as AAVrh.10BevMab or PBS. Mice were sacrificed at 4 wk. **A.** Hematoxylin and eosin staining (of representative mouse brains) of tumor and tumor tissue in PBS *vs* AAVrh.10BevMab-treated brain. Arrow indicates location of needle insertion for GBM implantation and therapy administration. Dashed circle outlines approximate area of GBM tumor. **B.** Immunohistochemical staining of $CD31^+$ endothelial cell (anti-CD31, green) in tumor and normal tissue (indicated by dashed line) in PBS (**left panels**) *vs* AAVrh.10BevMab-treated (**right panels**) mice bar = 100 µm. Higher magnification in bottom panels, bar = 50 µm. Yellow arrows indicate area of CD31+ staining, and *denotes area of endothelial vascularization. **C.** Blood vessel density in normal and U87MG tumor tissue of PBS *vs* AAVrh.10BevMab-treated mice. Quantification of GBM tumor angiogenesis was assessed as blood vessel density/area at 4 wk using $CD31^+$ endothelial cell quantification.

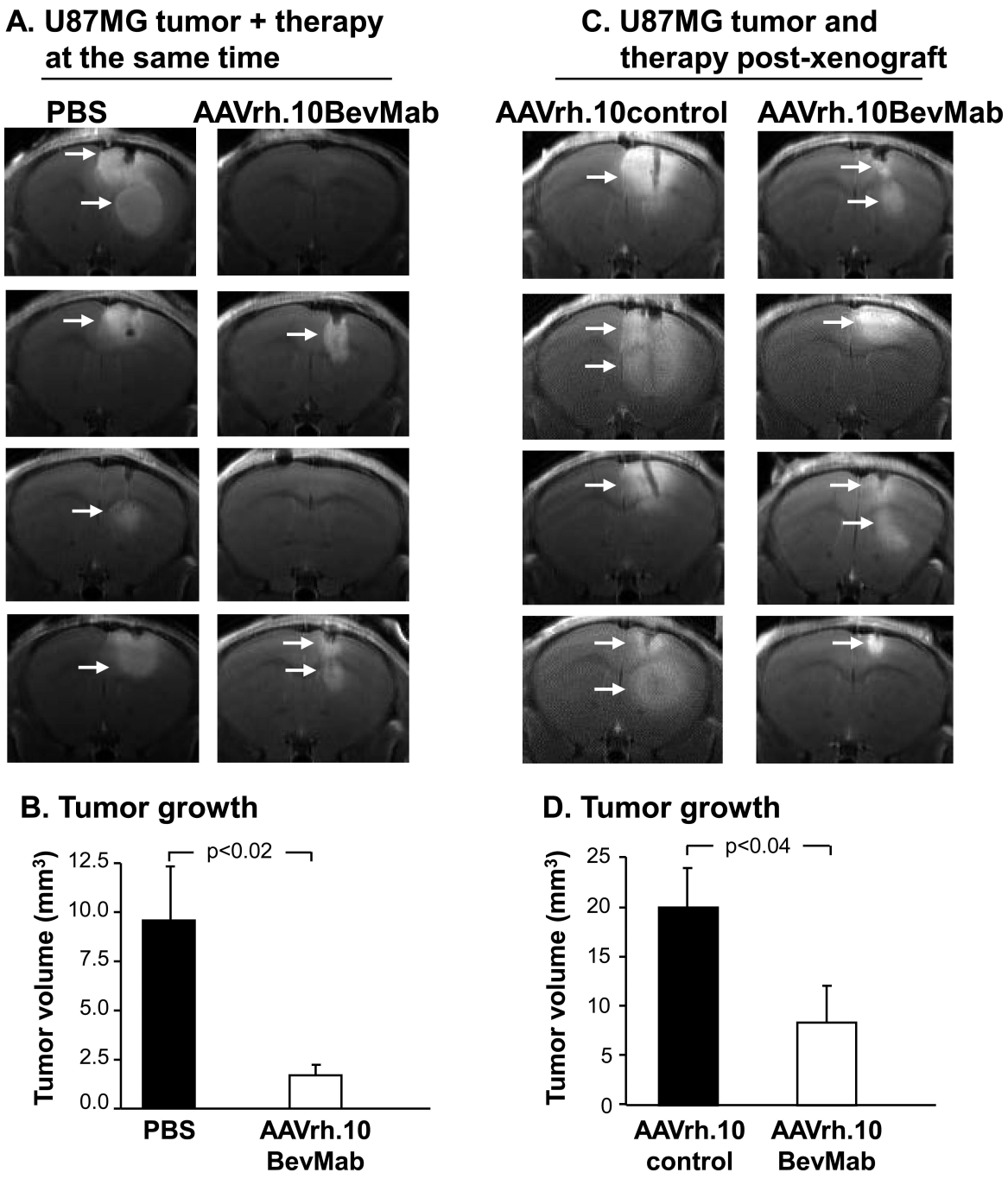

Figure 3.

MRI Assessment of tumor volume of mice with U87MG glioblastoma treated with AAVrh.10BevMab or control. U87MG and AAVrh.10BevMab was administered simultaneously (**A,B**) or 6 days after xenograft (**C,D**). In **A** and **C**, arrows indicate site of tumor on representative coronal image of striatum. Each coronal MRI image corresponds to site of xenograft implantation in four distinct mice. **A.** MRI, PBS-treated control mice (n=4) and AAVrh.10BevMab-treated mice (n=4). The scans were done at 18 days after U87MG implantation **B.** Quantification of tumor volumes (from multiple coronal MRI images of

whole brain), PBS-treated control (n=4) *vs* AAVrh.10BevMab-treated mice (n=4) at 18 days. **C**. MRI, PBS-treated control mice (n=4) and AAVrh.10BevMab post-xenograft treated mice (n=4). The scans were done at 20 days after U87MG implantation **D.** Quantification of tumor volumes in PBS *vs* post-xenograft treated mice (n=4 per group) at 20 days.

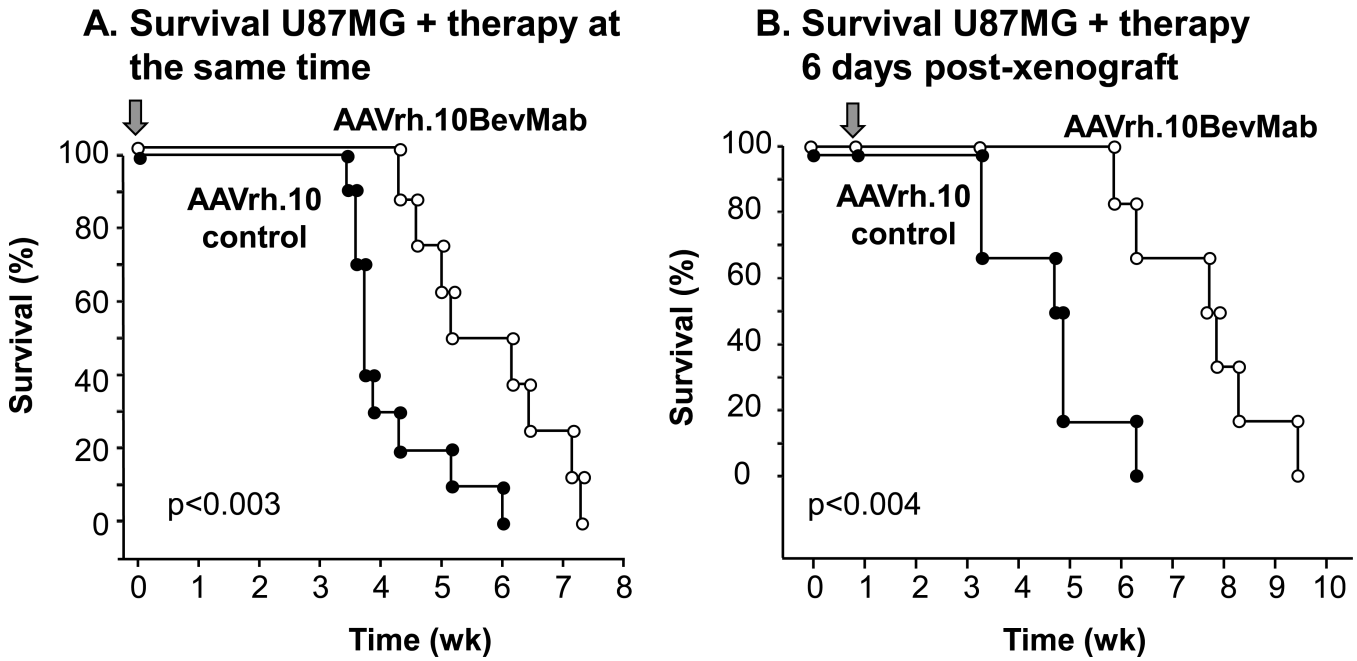

Figure 4.

Survival of mice with U87MG human glioblastoma xenografts treated with AAVrh.10BevMab. **A**. Survival of Mice treated simultaneously with AAVrh.10 control (n=9) or AAVrh.10BevMab (n=9). **B.** Survival of mice with U87MG human glioblastoma xenografts treated post-xenograft with AAVrh.10control (n=6) or AAVrh.10BevMab (n=6). Arrow indicates time of treatment.

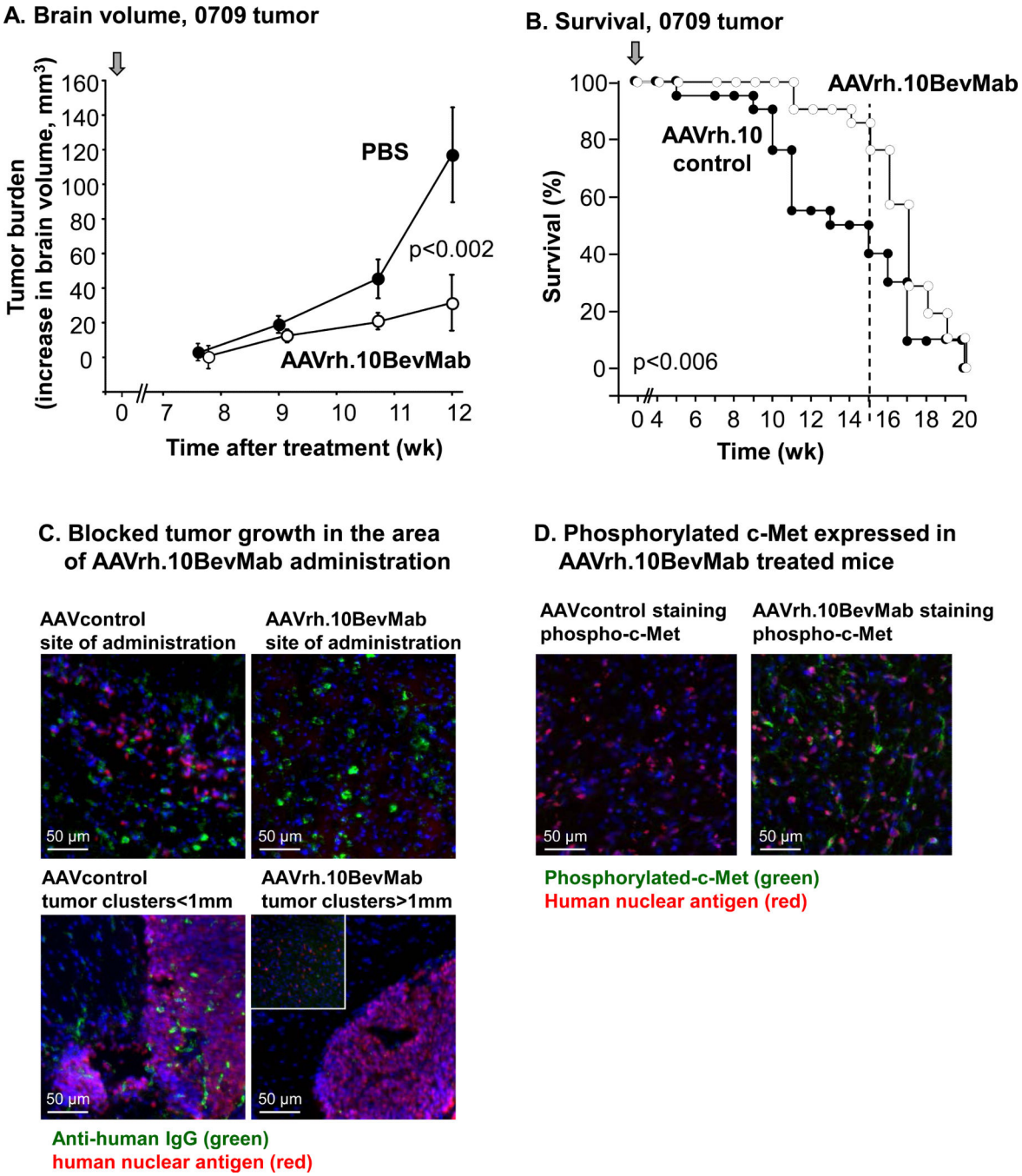

Figure 5.

Assessment of tumor burden and survival of mice with low-passage 0709 primary human glioblastoma following treatment with AAVrh.10BevMab. **A.** MRI quantification of tumor burden over time for PBS control (n=3) *vs* AAVrh.10BevMab-treated (n=3) mice. **B.** Survival of mice with xenografts treated simultaneously with AAVrh.10BevMab (n=21) or AAVrh.10control (n=21). For **A** and **B**, arrow indicates time of treatment. **C.** Immunofluorescent assessment of brains with #0709 GBM xenograft treated with AAVrh.10 control *vs* AAVrh.10BevMab (n=3). AAVrh.10BevMab-directed expression of

bevacizumab (and AAVrh.10control-directed expression of control antibody) was assessed with anti-human IgG antibody (anti-IgG, green), 0709 GBM tumor cells were assessed with anti-human nuclear antigen (HNA, red). **Top left panel**, AAVrh.10control-directed expression of control antibody (anti-IgG, green) in the area of 0709 tumor growth (HNA, red). **Top right panel,** AAVrh.10BevMab-directed expression of bevacizumab (anti-IgG, green) in the area of administration, tumor cells were not detected. **Bottom left panel**, #0709 tumor cell clusters (HNA, red) detected in areas of AAVrh.10control administration and expression (anti-IgG, green). **Bottom right panel**, #0709 tumor cell clusters (HNA, red) detected only at distance greater than 1mm from area of AAVrh10BevMab administration (not detected). bar = 50 μm**. D.** Immunohistochemical analysis of phosphorylated c-Met in AAVrh.10BevMab-treated primary tumors (n=3). L**eft panel**, #0709 tumor cell (HNA, red) detected AAVrh.10control treated mice, phospho-c-Met not detected.**Right panel**, #0709 tumor cell (HNA, red) detected along with phosphor-c-Met (anti-c-MET, green) in AAVrh10BevMab treated mouse brain. bar = 50μm.